Available online at www.sciencedirect.com

ScienceDirect

IFAC PapersOnline CONFERENCE PAPER ARCHIVE

IFAC PapersOnLine 59-1 (2025) 403–408

Model-based Optimization for Laboratory-Scale Upstream Processing in Monoclonal Antibody Production

Guilherme A. Pimentel [*] **Camilo Garcia-Tenorio** [*]
Radhouane Fekih-Salem [*,****] **Cédric Toussaint** [**] **Ahmed Kanfoud** [**]
Thomas Cornet [**] **Thibault Helleputte** [**] **Adrien Boes** [***]
Riccardo Marega [***] **Alain Vande Wouwer** [*] **Laurent Dewasme** [*]

[*] *Systems,Estimation,Control and Optimization Group, University of Mons, Belgium (e-mail: guilherme.araujopimentel@umons.ac.be)*
[**] *DNAlytics, Ottignies-Louvain-la-Neuve, Belgium*
[***] *Immunobiology Laboratory, CER Groupe, Belgium*
[****] *University of Tunis El Manar, National Engineering School of Tunis, LAMSIN, Tunisia*

Abstract: The production of monoclonal antibodies (mAbs) is a complex pharmacological process involving upstream and downstream chains, focusing on mAbs production and purification, respectively. This paper presents a process optimization based on an end-to-end mechanistic model for the upstream process chain to enhance the production of mAbs. Upstream processing considers cell expansion, cell production, and primary harvesting steps by filtration. The optimization results offer users the optimal initial concentrations of the medium in the bioreactors, the duration of the cultures, the feed flow rate profiles, and the permeate flow profile in the filtration operation. Simulations incorporating interconnected reactors and process constraints led to optimized initial media concentrations and feed flow profiles, resulting in a 25% increase in mAb production compared to baseline conditions.

Keywords: process optimization, monoclonal antibodies, upstream processing, mechanistic modeling.

1. INTRODUCTION

Creating novel pharmaceutical entities depends significantly on conducting small-scale wet laboratory experiments to identify the specific manufacturing conditions that result in the highest process yield and the best product quality. These efforts encompass a spectrum of activities, ranging from the modification of cell lines to the adjustment of culture media, operating conditions, and process configurations. In the last decades, significant advancements have been made in optimizing upstream processing (USP). Through the development of recombinant technologies, as well as media and process control strategies, there has been a remarkable increase in process efficiency, viable cell densities, and product titers in cell culture processes (Gronemeyer et al., 2014). These accomplishments were primarily the result of extensive laboratory experiments conducted as part of large-scale campaigns.

One way to reduce the number of experiments is to rely on models that mimic the processes, sparing time from the bench to production while minimizing the costs and environmental impact (Zobel-Roos et al., 2019). In addition, an end-to-end upstream process model provides a global understanding of the chain, anticipating the consequence of parameter changes from one step to another and, therefore, considering a global process optimization rather than an isolated optimization of each operation. However, the interconnections among units contribute to the complexity of the overall operational dynamics and the corresponding optimization problem. Additionally, recommended operating conditions and variables for a tailor-made pharmaceutical upstream process (for mAb production) are challenging to obtain because this situation often requires a certain level of customization. For instance, studies on the production of therapeutic proteins consider an oversimplified process setup, either considering only a batch bioreactor (Kornecki and Strube, 2019; Pimentel et al., 2022) or only fed-batch bioreactors (Badr et al., 2021; Wahlgreen et al., 2022). To the best of the authors' knowledge, none of the published studies consider preliminary harvesting steps, which prepare the culture for downstream processing, nor the complete setup, with cell expansion, cell production, flocculation, and filtration.

Given the abovementioned points, this paper proposes a model for a small-scale laboratory bench upstream chain process that encompasses cell expansion, cell production, and primary harvesting steps via filtration. Subsequently, process optimization is employed to establish the initial concentrations of the media in the bioreactors, the duration of the cultures, the feed flow rate profiles, and the permeate flow profile in the filtration operation to maximize monoclonal antibody (mAb) production.

This paper is organized as follows. Section 2 describes the lab-scale upstream process and its operating variables. Section 3 presents a mechanistic model for each process unit. Section 4 discusses the selection of the cost function to optimize the process and the operating conditions to maximize mAb production. Conclusions are drawn in Section 5, ending with work perspectives.

10.1016/j.ifacol.2025.03.069

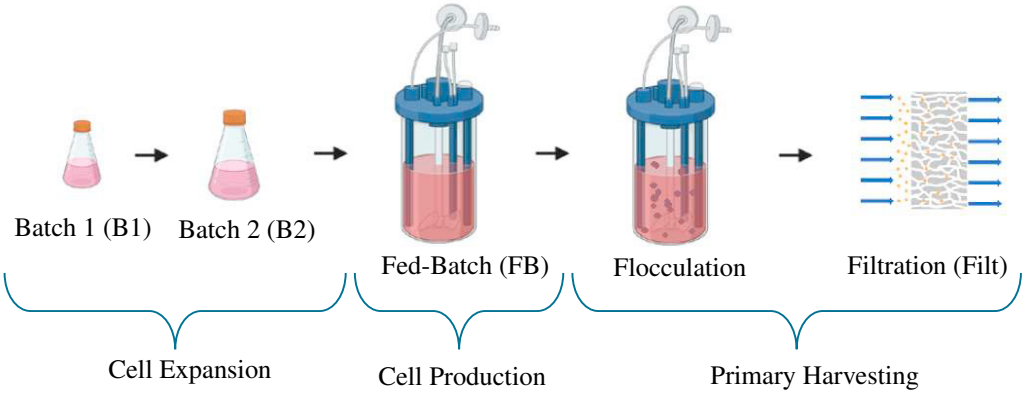

Fig. 1. Scheme of the generic upstream process for producing therapeutic proteins.

2. UPSTREAM PROCESSING SCHEME

The upstream processing stage is crucial since, based on the preparation and the manipulation of biological materials, it determines mAb production yield and productivity undergoing downstream processing. Accurate control of growth conditions such as temperature, pH, dissolved oxygen, and nutrient supply is required to ensure optimal cell growth and mAb production. The success of this step significantly impacts the quality, quantity, and efficiency of the final products (Jain and Kumar, 2008).

Figure 1 illustrates the upstream process chain, which generally consists of three phases: (i) cell expansion, (ii) cell production, and (iii) primary filtration or harvesting. Cell expansion involves the upscaling growth of mammalian cells in batch mode. Cell production is responsible for achieving the desired process targets, such as cell viability and product (mAb) titer, and is typically carried out in a fed-batch bioreactor. The final phase, primary filtration, prepares the production for the downstream process by extracting impurities generated in the upstream steps.

3. UPSTREAM MECHANISTIC MODELING

As previously mentioned, the upstream process scheme mainly comprises bioreactors to create a favorable environment to produce the desired therapeutic product. This study uses the framework of mechanistic representation of macroscopic bioreactions.

Mammalian cells predominantly use glucose as their primary carbon source and produce lactate as a byproduct. However, when there is a low glycolysis rate (glucose consumption rate) and a high lactate concentration, cells are likely to adjust their metabolism by increasing lactate consumption to compensate for the lack of glucose. This process can be represented by a three-reaction model as follows (Pimentel et al., 2023):

$$k_{31}G + Gn \xrightarrow{\varphi_1} k_{11}X_v + k_{51}L + k_{61}mAb \tag{1a}$$

$$k_{52}L \xrightarrow{\varphi_2} X_v \tag{1b}$$

$$k_{13}X_v \xrightarrow{\varphi_3} X_d + k_{63}mAb \tag{1c}$$

where the concentrations of viable biomass reads X_v, dead biomass as X_d, glucose as G, glutamine as Gn, lactate as L, and monoclonal antibody as mAb. The first reaction involves substrate consumption (glycolysis) to produce biomass and byproducts, with a rate φ_1. The second reaction consists of the consumption of lactate to generate viable biomass, governed by φ_2. The last reaction represents biomass decay, leading to the production of dead biomass and the release of mAbs into the medium. The ordinary differential equation system related to (1) reads:

$$\frac{dX_v}{dt} = k_{11}\varphi_1 + \varphi_2 - k_{13}\varphi_3 - DX_v, \tag{2a}$$

$$\frac{dX_d}{dt} = \varphi_3 - DX_d, \tag{2b}$$

$$\frac{dG}{dt} = -k_{31}\varphi_1 - D(G - G_{in}), \tag{2c}$$

$$\frac{dGn}{dt} = -\varphi_1 - D(Gn - Gn_{in}), \tag{2d}$$

$$\frac{dL}{dt} = k_{51}\varphi_1 - k_{52}\varphi_2 - DL, \tag{2e}$$

$$\frac{dmAb}{dt} = k_{61}\varphi_1 + k_{63}\varphi_3 - DmAb,, \tag{2f}$$

$$\frac{dV}{dt} = F_{in}, \tag{2g}$$

with reaction rates as

$$\varphi_1 = \mu_{max,1}\frac{Gn}{(K_{Gn}+Gn)}\frac{G}{(K_G+G)}X_v, \tag{3a}$$

$$\varphi_2 = \mu_{max,2}\frac{L}{(K_L+L)}\frac{K_{GI}}{(K_{GI}+G)}X_v, \tag{3b}$$

$$\varphi_3 = \mu_{dmax}\frac{K_{Gnd}}{(K_{Gnd}+Gn)}X_v, \tag{3c}$$

where k_{ij} are the stoichiometric coefficients, K_{Gn}, K_G, K_L are the half-saturation parameters, $\mu_{max,1}$, $\mu_{max,2}$, and μ_{dmax} the maximum reaction rate parameters, and K_{GI} and K_{Gnd} the inhibition parameters. The reaction rate φ_1 is driven by two Monod factors activated by glucose and glutamine. Likewise, φ_2 stands for the selective consumption of lactate activated by lactate and inhibited by glucose (i.e., glucose is assumed to be the preferential substrate). φ_3 models the biomass death rate inhibited by the presence of glutamine, which is the primary nitrogen source of the cell, ensuring its viability. The fed-batch model comprises the dilution rate, which is a transport term computed as $D = F_{in}/V$, where F_{in} is the feed flow containing specific and usually high glucose (G_{in}) and glutamine (Gn_{in}) concentrations. When the bioreactor is operated in batch mode, the feed flow is zero $F_{in} = 0$, which keeps the bioreactor at a constant volume ($\frac{dV}{dt} = 0$), and the dilution rate at zero, $D = 0$.

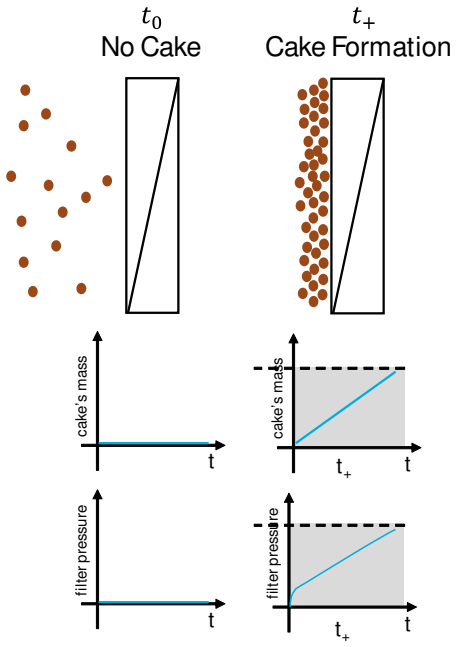

Fig. 2. Dynamical behavior of the cake formation and transmembrane pressure when the permeate flow is set to a constant value. t_0 and t_+ stand for the instants respectively preceding and following the pump actuation (gray area).

Following the production phase, a separation process cleans impurities residing along with the biopharmaceutical product itself. This step prepares the medium with the produced compound for downstream processing. First, a flocculation agent is added to the reactor, where negatively charged particles such as cells, cellular debris, nucleic acids, and host cell proteins (HCPs) bind to positively charged polymers, leaving the protein of interest in the solution. This step is critical for the following step of filtration.

Flocculation occurs on a timescale of minutes, whereas cell growth occurs over days. Therefore, it is reasonable to decouple the kinetics using a so-called slow-fast hypothesis. The flocculation efficiency is modeled as an α factor, deciding which particles will be present in the permeate after the filtration step. The filtration process is driven by a time-varying permeate flux profile and a transmembrane pressure which increases as impurities accumulate and form a layer (called "cake") represented in Figure 2.

The relation between permeate flow and filter pressure is modeled by

$$\Delta P = J_v \cdot \eta_0 \cdot R_{total}, \tag{4}$$

where J_v $[L/(h \cdot m^2)]$ is the permeate flux, ΔP $[Pa]$ is the measured pressure variation applied to the filter, η_0 $[Pa \cdot h]$ is the medium dynamic viscosity. The total filter resistance $[1/m]$ is described by

$$R_{total} = R_m + R_{cake}, \tag{5}$$

where $R_m[1/m]$ is the resistance of the filter membrane, and the resistance of the membrane cake is represented as follows:

$$R_{cake} = \rho \left(\frac{m_0}{A_{filt}} + m_{perm} \right), \tag{6}$$

where ρ $[m/10^6 Cells]$ is the specific cake resistance, A_{filt} $[m^2]$ is the filter area and m_0 $[10^6 Cells]$ is the cake initial mass. The dynamic behavior of cake formation is modeled using similar principles as in (Pimentel et al., 2015):

Table 1. Model parameters.

B1, B2 and BF model		Filtration model	
Parameter	Value[1]	Parameter	Value
$\mu_{max,1}$ $[g/(10^9 Cells\ d))]$	0.460	R_m $[m^{-1}]$	1.1236×10^5
$\mu_{max,2}$ $[g/(10^9 Cells\ d))]$	0.400	A_{filt} $[m^2]$	0.0022
μ_{dmax} $[d^{-1}]$	0.03	η_0 $[Pa \cdot h]$	2.492
K_G $[g/L]$	1.10	m_0 $[10^6 Cells]$	0.00
K_{Gn} $[g/L]$	0.250	ρ $[m/10^6 Cells]$	0.2
K_L $[g/L]$	1.20	α	0.95
K_{GI} $[g/L]$	0.800		
K_{gnd} $[g/L]$	0.002		
k_{11} $[(10^9 Cells/g)]$	6.80		
k_{31} $[g/g]$	18.0		
k_{51} $[g/g]$	10.70		
k_{52} $[g/g]$	1.20		
k_{61} $[mg/g]$	107.80		
k_{63} $[mg/g]$	2.90		

[1] values from Pimentel et al. (2023).

$$\frac{dX_{perm}}{dt} = J_v(1-\alpha)X_{total}, \tag{7a}$$

$$\frac{dm_{perm}}{dt} = J_v \alpha X_{total}, \tag{7b}$$

$$\frac{dV_{perm}}{dt} = J_v, \tag{7c}$$

where X_{total} $[10^6 Cells/mL]$ is the concentration of total suspended solids in the media, α is the efficiency of the flocculation operation, X_{perm} $[10^6 Cells/m^2]$ are the cells that pass through the filter, m_{perm} $[10^6 Cells/m^2]$ are the cells retained by the filter and V_{perm} $[L/m^2]$ is the filter volumetric throughput.

4. UPSTREAM OPTIMIZATION

The optimization methodology will be implemented in the two main stages of the upstream process: (i) cell expansion/production and (ii) primary harvesting. For the first stage, the objective is to find a parameter vector θ_{Prod} that optimizes the process variables of the (fed-)batch bioreactors, such as initial concentrations in the reactors, the inlet feed medium concentration and flow rate profile, and the culture duration. For the second stage, the optimization returns θ_{Filt} containing the time-series profile of the permeate flow rate while keeping the filtration pressure below a predefined value. Then, the optimization problem for either case can be expressed as follows:

$$\theta_i = \arg\min_{\theta_i} \mathcal{F}(\theta_i) : \bar{\theta}_i < \theta_i < \underline{\theta}_i, \tag{8}$$

where the solutions of θ_i for $i = [Prod, Filt]$ are constrained in upper- and lower-bounds that are defined as maximal concentrations and duration of the batch and fed-batch cultures and minimal and maximal pump flow rate on the permeate flow.

4.1 Optimization - Cell Expansion and Production

Before implementing the optimization strategy, a simulation that considers predefined operation conditions is carried out as a baseline. The simulation considers model (2) with full-state measurements at a sampling time of $t_s = 0.25$ *days*. Also, the measurements are corrupted by independent and identically distributed (IID) Gaussian noise $e \sim (0, \sigma^2)$. The imposed variances are 0.1×10^6Cells/mL, 0.01×10^6Cells/mL,

Table 2. Results of the optimization problem for B1, B2 and FB.

Optimal Batch 1			Optimal Batch 2			
$G_{0,B1}$ $[g/L]$	$Gn_{0,B1}$ $[g/L]$	endB1 [d]	$G_{0,B2}$ $[g/L]$	$Gn_{0,B2}$ $[g/L]$	endB2 [d]	
0.3871	0.3027	2.500	0.4409	0.4713	5.250	
Optimal Fed-Batch						
$G_{0,FB}$ $[g/L]$	$Gn_{0,FB}$ $[g/L]$	G_{in} $[g/L]$	Gn_{in} $[g/L]$	endFB [d]	$\lambda[-]$	$\beta[-]$
0.9552	0.2546	3.527	1.957	8.752	0.0012	0.0574
Cost function weights						
w_G	w_{Gn}	$w_{X_{v,B2}}$	$w_{t_{B1}}$	$w_{X_{v,FB}}$	w_V	
0.01	0.01	50	45	0.10	2000	
Lower Bounds						
$\underline{\theta}_{G_{0,B1}}$ $[g/L]$	$\underline{\theta}_{Gn_{0,B1}}$ $[g/L]$	$\underline{\theta}_{endB1}[d]$	$\underline{\theta}_{G_{0,B2}}$ $[g/L]$	$\underline{\theta}_{Gn_{0,B2}}$ $[g/L]$	$\underline{\theta}_{endB2}[d]$	
0.0070	0.0006	2.000	0.0070	0.0006	2.000	
$\underline{\theta}_{G_{0,FB}}$ $[g/L]$	$\underline{\theta}_{Gn_{0,FB}}$ $[g/L]$	$\underline{\theta}_{G_{in}}$ $[g/L]$	$\underline{\theta}_{Gn_{in}}$ $[g/L]$	$\underline{\theta}_{endFB}[d]$	$\underline{\theta}_{\lambda}[-]$	$\underline{\theta}_{\beta}[-]$
0.0070	0.0006	0.0070	0.1000	2.000	0.000	0.000
Upper Bounds						
$\bar{\theta}_{G_{0,B1}}$ $[g/L]$	$\bar{\theta}_{Gn_{0,B1}}$ $[g/L]$	$\bar{\theta}_{endB1}[d]$	$\bar{\theta}_{G_{0,B2}}$ $[g/L]$	$\bar{\theta}_{Gn_{0,B2}}$ $[g/L]$	$\bar{\theta}_{endB2}[d]$	
8.400	0.6960	10.00	8.400	0.6960	10.00	
$\bar{\theta}_{G_{0,FB}}$ $[g/L]$	$\bar{\theta}_{Gn_{0,FB}}$ $[g/L]$	$\bar{\theta}_{G_{in}}$ $[g/L]$	$\bar{\theta}_{Gn_{in}}$ $[g/L]$	$\bar{\theta}_{endFB}[d]$	$\bar{\theta}_{\lambda}[-]$	$\bar{\theta}_{\beta}[-]$
8.400	0.6960	10.00	2.000	10.00	1.000	1.000

0.05 g/L, 0.01 g/L, 0.2 g/L, and 5.0 μg/mL for viable biomass X_v, dead biomass X_d, glucose G, glutamine Gn, lactate L, and mAb, respectively. Table 1 shows the values of the model parameters previously identified at lab-scale in Pimentel et al. (2023).

The cell expansion phase is modeled by (2) with $F_{in} = D = 0$, as represented in Figure 1. Batch reactor 1 (B1) is set with a working volume of 10mL and inoculum concentration of $X_{v0,B1} = 0.9 \times 10^6 Cells/mL$, the initial concentration of dead biomass, lactate, and mAb are zero ($X_{d0,B1} = L_{0,B1} = mAb_{0,B1} = 0$). The initial glucose concentration is 6.0 g/L, and glutamine is 0.58 g/L in all bioreactors initial conditions. The processes are interrupted when one of the substrates is consumed completely.

B1 is interconnected to another batch mode reactor, B2, with a working volume of 200mL. The initial concentration of B2 is the final concentration achieved by B1, considering the dilution to the larger volume. As batch B1 consumes most substrates, new media with glutamine and glucose are added in B2 to reach the same initial concentration for glucose and glutamine of B1.

After the cell expansion phase, 50 ml of the culture of B2 is used to start the production operation in a fed-batch bioreactor with a maximum working volume of 800mL. The 50ml are added in a 350ml fresh medium ($V_{0,FB} = 400mL$ with concentration of $G_{0,FB} = 6.0\ g/L$, and glutamine is $Gn_{0,FB} = 0.58\ g/L$. The fed-batch process is modeled by (2) with $F_{in} \neq 0$.

Fed-batch operation typically avoids substrate depletion, which may cause biomass decay, by feeding fresh medium into the bioreactor. For instance, in this study, a pulse with medium concentrations of 5 g/L of glucose and 1.12 g/L of glutamine is added to the process around day 13, when glutamine is almost exhausted and viable biomass decreases. A second pulse is required around day 14 for the same reason. It is important to highlight that the selection of the number of pulses, related substrate quantities, and medium concentrations, relies on a sequence of expensive wet laboratory experiments where all possible combinations are tested. In the present case, we use the fresh medium concentrations provided by these tests. Simulation results using these values are shown by the dashed lines in Figures 3 and 4.

Consequently, to overcome the difficulty of defining media concentrations and feed-flow rates, the model-based optimization of the process is used. In summary, the objective of the optimization problem is to obtain the initial concentrations of the medium for glucose and glutamine B1, B2, and FB ($G_{0,B1,B2,FB}$ and $Gn_{0,B1,B2,FB}$). In addition, it finds the optimal duration for all the cultures (endB1, endB2, and endFB). The feed flow rate for the fed-batch mode normally has three operation values to design: glucose and glutamine concentrations (G_{in} and Gn_{in}), and the feed flow rate profile F_{in}, considered as exponential and defined by:

$$F_{in} = \beta e^{\lambda t_{BF}}, \tag{9}$$

where the profile parameters β and λ as well as the culture duration t_{BF} are to determined. The decision vector, therefore reads:

$$\theta_{Prod} = [G_{0,B1}\ \ Gn_{0,B1}\ \ endB1\ \ G_{0,B2}\ \ Gn_{0,B2}\ \ endB2\ \ G_{0FB}\ \ Gn_{0FB}\ \ G_{in}\ \ Gn_{in}\ \ endFB\ \ \lambda\ \ \beta]. \tag{10}$$

To meet the objectives of the cell expansion and production optimization, the following cost function is defined:

$$\begin{aligned} \mathcal{F}(\theta_{Prod}) = {} & w_G \cdot (G_{B1,B2,FB}(0)) + \\ & w_{Gn} \cdot (Gn_{B1,B2,FB}(0)) + \\ & -w_{X_{v,B2}} \cdot (X_{v,B2}(endB2)) + \\ & -w_{X_{v,FB}} \cdot (X_{v,FB}(endFB)) + \\ & w_V \cdot (V_{set} - V_{FB}(endFB)) + \\ & -w_{t_{B1}} \cdot endB1, \end{aligned} \tag{11}$$

where the first and the second objectives are to use the minimum possible initial concentrations of glucose and glutamine in the medium of all bioreactors. The third and fourth terms maximize the production of viable biomass in Batch 2 and the production phase (FB). The working volume of the FB phase is also maximized while minimizing the duration of B1. The contribution of each term can be scaled using the weights w_i ($i = G,\ Gn,\ X_{v,B2},\ X_{v,FB},\ V,\ t_{B1}$). The solution is obtained by solving the constrained nonlinear multivariable function $\mathcal{F}(\theta_{Prod})$ using `fmincon()` function of Matlab with a fixed-step solver `ode3` (Bogacki-Shampine Formula integration technique), where the upper and lower bounds are inspired by the laboratory scale trials for the cell expansion and production reported in Pimentel et al. (2023). The values of the upper- and lower-bounds are presented in Table 2.

Table 2 also presents the obtained concentration, duration, and feed parameters, considering that the cost function weights were chosen to prioritize the maximization of viable biomass while minimizing medium consumption. Constraints on glucose concentrations ensure that substrate inhibition effects were mitigated.

Figure 3 shows, in solid lines, the dynamic evolution of the process variables and the maximization of the viable biomass concentration in the production phase, which consequently leads to the expected maximization of the cell production and mAbs.

The solution of (8) considering (10) and the cost function (11) presents interesting features of the process. First, the duration of the batches, as expected, can be linked to the exponential phase duration of the process. Compared to the non-optimal case, it is important to highlight that even though the duration of B1 and B2 are longer, this does not significantly affect the initial concentration in the production phase.

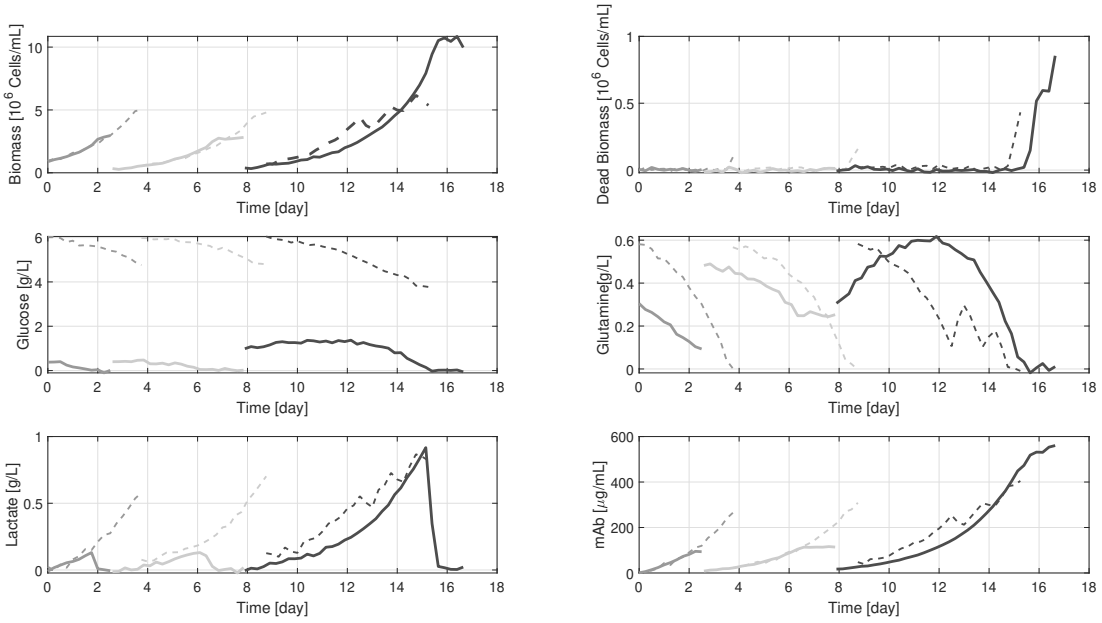

Fig. 3. Time profiles of viable biomass, dead biomass, glucose, glutamine, lactate, and protein concentrations during the B1 (gray), B2 (light-gray), and fed-batch (black) cultures. Solid lines are the optimized process. Dashed-line the pulse of glucose and glutamine.

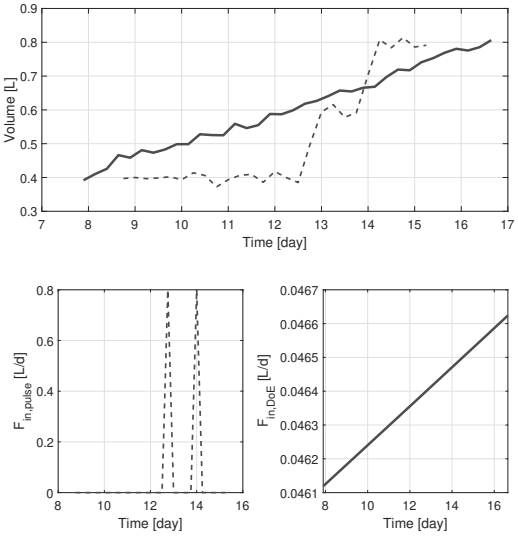

Fig. 4. Inlet flow (F_{in}) and volume corrupted by measurement noise. Solid lines are the optimal solution. Dashed-line the pulse of glucose and glutamine.

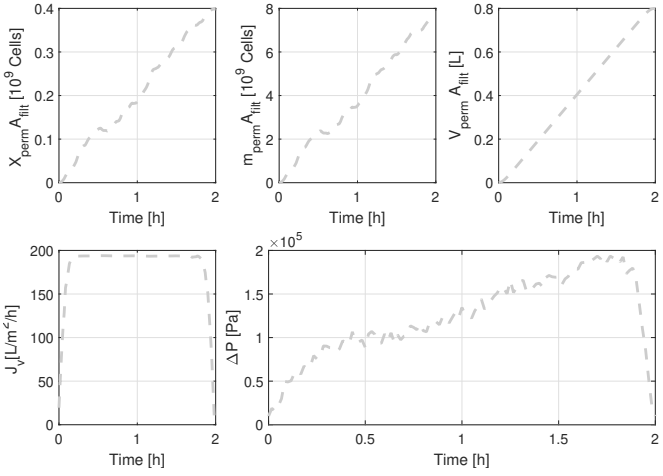

Fig. 5. Results of the optimization problem of the filtration considering the maximum pressure of $2.0 \times 10^5 Pa$ (2 bar).

Another interesting point is that, unlike the non-optimal results, which present a high concentration of lactate, the optimized process consumes lactate, which extends the duration of the process and also contributes to maximizing viable biomass production when the exponential phase ends.

Furthermore, all the glucose and glutamine are completely used up, indicating an efficient use of the consumables. Finally, another mechanism contributing to the increase in the production of mAbs is the occurrence of biomass death in the last days of the production phase, which is expressed by reaction (1c). Figure 4 presents the feed profile F_{in}, which almost remains constant during the fed-batch phase, most probably because the concentration G_{in} and Gn_{in} have been optimized. To measure the optimization level, the values of the cost function (11) for both scenarios have been computed. The non-optimal case yields a value of 19.046, while the optimal design implementation results in a significantly improved value of 7.266. This improvement can be attributed to the reduced use of consumables and the increased production of viable biomass.

4.2 Optimization - Primary Harvesting

As highlighted in Figure 1, primary harvesting comprises two operations: the flocculation and the filtration. This study assumes flocculation as a static process with an efficiency represented by α. During the process, the biomass flocculates and is blocked by the filter pores while the remaining medium containing mAbs goes through. Thus, the filter gets clogged with time because of the accumulation of these biomass flocs, which increases the transmembrane pressure in the filter.

Table 3. Weights of the optimization problem for filtration.

Cost function weights		
w_{smooth}	$w_{\Delta P}$	$w_{V_{filt}}$
0.1	0.001	200

The filtration is modeled by (7) with a membrane area of $0.0022m^2$ and flocculation efficiency of $\alpha = 0.95$ where the total solids in the culture $X_{total} = X_{v,FB}(endFB) + X_{d,FB}(endFB)$. The permeate volume is the same as the maximum volume of the production phase, $V_{filt,set} = 800mL$.

Simulations of the filtration consider the models (4) - (7) where the measurements of permeate filtration and the membrane are used. To be more realistic, an independently and identically distributed (IID) Gaussian noise $e \sim (0, \sigma^2)$ corrupts the measurements. X_{total} is assumed to present a variance of $10 \times 10^6 Cells$, resulting from measurement uncertainties on $X_{v,FB}$ and $X_{d,FB}$ biomass populations following the flocculation operation. In addition, a variation in the pressure measurement of 0.1×10^5Pa is also considered. All the simulation parameters are reported in Table 1.

The optimization is achieved by solving (8) and delivers:

$$\theta_{Filt} = [j_{v,1} \;\; j_{v,2} \;\; \cdots \;\; j_{v,N_{filt}}], \tag{12}$$

where $j_{v,i}$ is the value for each instant of the permeate flow J_v and the N_{filt} is the maximum sample number. To obtain the optimal permeate flow profile J_v, two hard constraints are imposed: (i) the dosing pump which ranges from 0.01 mL/min to 10 mL/min, and (ii) the maximum pressure allowed set to 2.0×10^5 Pa. The cost function eventually reads:

$$\begin{aligned} \mathcal{F}(\theta_{Filt}) = w_{V_{filt}} \cdot \big(V_{filt,set} - V_{filt}(endFilt)\big) + \\ w_{\Delta P} \cdot (max(\Delta P(k))) + \\ w_{smooth} \cdot (J_{V,smooth}), \end{aligned} \tag{13}$$

where the smoothness term is computed as

$$J_{V,smooth} = \sum_{k=0}^{n-1} (\hat{J}_{v,k+1} - \hat{J}_{v,k})^\top \cdot (\hat{J}_{v,k+1} - \hat{J}_{v,k}). \tag{14}$$

The filtration of the total volume should be achieved while keeping the pressure below $2.0 \times 10^5 Pa$, and obtaining a smooth permeate flow profile. A sampling time of 1 minute ($t_{s,filt} = 0.016h$) is considered, as well as a total filtration duration of two hours ($endFilt = 2h$). Table 3 presents the design of the weights based on the measurement magnitudes.

Figure 5 presents the dynamic optimal profile of the permeate flow J_v. Note that the relation between the maximum pressure and the permeate flow is computed using relation (4), where the total filtration resistance evolves with the cell spreading over the filter surface m_{perm}. The permeate composition is represented by X_{perm} and the concentration of the mAbs obtained at the end of the production operation. Despite the X_{total} and the pressure noisy measurements, the permeate flow J_v profile computed by the optimization problem presents a smooth trajectory, which is mainly due to the addition of the term (14).

5. CONCLUSION

This work investigates the integration of mechanistic modeling to effectively optimize the upstream process operational variables. The findings demonstrate an effective utilization of consumables and a considerable rise in monoclonal antibody (mAb) concentration during the production phase compared to the non-optimal case. The optimization procedure accounts for various operational variables, including initial concentrations and batch durations, feed profiles, durations, and media concentrations, as well as permeate flux profile, taking into consideration hard constraints such as minimal and maximal pump flow rates and filtration pressure. Future work will focus on experimental validation of the model and exploration of the impact of protein retention during filtration.

ACKNOWLEDGEMENTS

The authors acknowledge the support of the NEMO project (convention 8722) of the Biowin Walloon cluster achieved in collaboration with the CER Groupe, DNAlytics, and UCB. The scientific responsibility rests with its authors.

REFERENCES

Badr, S., Okamura, K., Takahashi, N., Ubbenjans, V., Shirahata, H., and Sugiyama, H. (2021). Integrated design of biopharmaceutical manufacturing processes: Operation modes and process configurations for monoclonal antibody production. *Computers and Chemical Engineering*, 153(107422), 1–14.

Gronemeyer, P., Ditz, R., and Strube, J. (2014). Trends in upstream and downstream process development for antibody manufacturing. *Bioengineering*, 1, 188–212.

Jain, E. and Kumar, A. (2008). Upstream processes in antibody production: Evaluation of critical parameters. *Biotechnology Advances*, 26, 46–72.

Kornecki, M. and Strube, J. (2019). Accelerating biologics manufacturing by upstream process modelling. *Processes*, 7(166), 1–17.

Pimentel, G.A., Dewasme, L., Santos-Navarro, F.N., Boes, A., Côte, F., Filée, P., and Vande Wouwer, A. (2023). Macroscopic dynamic modeling of metabolic shift to lactate consumption of mammalian cell batch cultures. In *9th International Conference on Control, Decision and Information Technologies*.

Pimentel, G.A., Dewasme, L., and Vande Wouwer, A. (2022). Data-driven linear predictor based on maximum likelihood nonnegative matrix decomposition for batch cultures of hybridoma cells. In *13th IFAC Symposium on Dynamics and Control of Process Systems, including Biosystems DYCOPS 2022*.

Pimentel, G.A., Vande Wouwer, A., Harmand, J., and Rapaport, A. (2015). Design, analysis and validation of a simple dynamic model of a submerged membrane bioreactor. *Water Research*, 70, 97–108.

Wahlgreen, M.R., Meyer, K., Ritschel, T.K.S., Engsig-Karup, A.P., Gernaey, K.V., and Joorgensen, J.B. (2022). Modeling and simulation of upstream and downstream processes for monoclonal antibody production. *IFAC PapersOnLine*, 55(7), 685–690.

Zobel-Roos, S., Schmidt, A., Mestmäcker, F., Mouellef, M., Huter, M., Uhlenbrock, L., Kornecki, M., Lohmann, L., Ditz, R., and Strube, J. (2019). Accelerating biologics manufacturing by modeling or: Is approval under the QbD and PAT approaches demanded by authorities acceptable without a digital-twin? *Processes*, 7(2).